Bioresource Technology 155 (2014) 63–70

Contents lists available at ScienceDirect

Bioresource Technology

journal homepage: www.elsevier.com/locate/biortech

Slow pyrolysis of rice straw: Analysis of products properties, carbon and energy yields

Jinje Park[a], Yongwoon Lee[a], Changkook Ryu[a,*], Young-Kwon Park[b]

[a] School of Mechanical Engineering, Sungkyunkwan University, Suwon 440-746, Republic of Korea
[b] School of Environmental Engineering, University of Seoul, Seoul 130-743, Republic of Korea

HIGHLIGHTS

- Slow pyrolysis of rice straw was investigated for temperatures of 300–700 °C.
- Biochar had a mass yield of about 25% from the organic fraction above 500 °C.
- Biochar was the primary product containing 40% of energy and 45% of carbon.
- Bio-oil and light gases had about 60% of energy yield in total.
- Drying of raw material was crucial to efficiently utilize the gases for process heat.

ARTICLE INFO

Article history:
Received 7 November 2013
Received in revised form 15 December 2013
Accepted 18 December 2013
Available online 27 December 2013

Keywords:
Biochar
Carbon yield
Energy yield
Rice straw
Slow pyrolysis

ABSTRACT

Among many uses of rice straw, application of its biochar from pyrolysis to the soil is receiving greater interest for increased crop productivity and sequestration of CO_2. This study investigated slow pyrolysis of rice straw at 300–700 °C to characterize the yields and detailed composition of the biochar, bio-oil and non-condensable gases. Biochar was analyzed for pH, microscopic surface area and pore volume distribution. Although the mass yield for the organic fraction was only about 25% above 500 °C, biochar was the primary product of pyrolysis containing 40% of energy and 45% of carbon from the straw. The utilization of by-products (bio-oil and gases) as energy resources was essential, since the sum of energy yield was about 60%. The gases could be burned to produce the heat for an auto-thermal pyrolysis process, but the heat balance was significantly influenced by the moisture content of the raw material.

© 2013 Elsevier Ltd. All rights reserved.

1. Introduction

Biomass is composed of organic polymers originally produced by photosynthesis. Based on the available forms, biomass can be categorized into forestry/wood residues, agricultural residues, organic fractions of municipal/industrial wastes, manures, energy crops, and macro/micro algae. Biomass is unique among renewable energy resources, because it can be converted into both energy and chemical feedstock. Various mechanical, biological and thermo-chemical conversion technologies have been developed for the use of biomass, and applied in industry to produce different types of energy, fuel and chemical products. The thermo-chemical conversion includes pyrolysis, gasification and combustion.

Rice straw a major agricultural residue, accounting for 731 Tg/yr in the world (average of 1997–2001), mostly generated in Asia (Kim and Dale, 2004). In developed countries, rice straw is densified into bales by harvesters at paddy fields for easy transport and storage. It has many competing uses, such as cattle feed, bedding for poultry, compost and energy/chemical production. In under-developed countries, however, rice is manually harvested, and the straw is often left in the field and burned. For a large-scale energy production from rice straw, combustion is the dominant technology used in industry with a typical scale of 5–12 MWe (Gadde et al., 2008). However, the high SiO_2 and alkali metal content in the rice straw often cause problems, such as erosion in size reduction equipment and slagging/fouling in the heat exchangers of a boiler. It is also difficult to feed or to reduce its size due to its fibrous form.

Pyrolysis is an alternative technology for utilization of rice straw for conversion into valuable products. It involves the thermal decomposition of organic polymers that release vapors of various molecular weight compounds leaving carbon-rich solid residue (char) (Jahirul et al., 2012). The pyrolytic vapors can be separated into condensable hydrocarbon compounds (oil, also known as tar) and non-condensable gases. For biomass, it can be used as a

---

* Corresponding author. Tel.: +82 31 299 4841; fax: +82 31 290 5889.
E-mail address: cryu@me.skku.ac.kr (C. Ryu).

0960-8524/$ - see front matter © 2013 Elsevier Ltd. All rights reserved.
http://dx.doi.org/10.1016/j.biortech.2013.12.084

single-step conversion process dedicated to the production of biochar, bio-oil and gases for use as fuels or chemical feedstock. The process is also an initial step for further break-down of the organic polymers in an oxidative atmosphere during gasification or combustion processes. Pyrolysis characteristics (reaction kinetics, products yields and composition) are influenced by many parameters, such biomass types, temperature, heating rate, particle size, reaction atmosphere, and vapor residence time due to the complex chemical structures and reactions involved (Antal and Grønli, 2003).

Table 1 presents recent studies in literature for pyrolysis of rice straw. Fast pyrolysis technology has been investigated mainly for production of bio-oil. It is typically performed using a fluidized bed to increase the heating rate (~10^3 °C/s) and at temperatures about 500 °C to maximize the bio-oil yield (Wannapeera et al., 2008; Jung et al., 2008; Zhang et al., 2013; Eom et al., 2013; Pattiya and Suttibak, 2012; Fu et al., 2011, 2012; Lou et al., 2010). Higher temperatures and increased vapor residence time cause thermal cracking of hydrocarbon compounds, decreasing bio-oil yield. Pyrolysis using radio frequency plasma has been also studied to increase the gas yields by fully converting the tar (bio-oil) compounds to CO and H_2 rich gases (Tu et al., 2009).

In contrast to fast pyrolysis, slow pyrolysis is performed at a heating rate of about 10 °C/m for a typical temperature range of 300–700 °C (Pütün et al., 2004; Xiao et al., 2010; Peng et al., 2011; Huang et al., 2012, 2013; Wu et al., 2012; Chatterjee et al., 2013). This requires about 1 h of particle residence time to reach the target temperature. Slow pyrolysis of rice straw is applied as pretreatment (Xiao et al., 2010; Huang et al., 2012), or for biochar production as a soil ameliorator (Peng et al., 2011; Wu et al., 2012). Pyrolysis at low temperatures (typically below 300 °C), also referred to as torrefaction, is used to upgrade its fuel quality, such as the heating value (energy density) and grindability, as a pretreatment of biomass for pelletization, bio-oil production, gasification or combustion processes (Meng et al., 2012; Batidzirai et al., 2013).

Recent interest on slow pyrolysis of rice straw is for the application of biochar to soil to increase the soil fertility and to sequestrate carbon. Biochar increases the retention of nutrients and water in soil and provides habitats for symbiotic micro-organisms, which reduces the need for chemical fertilizers and increases crop productivity (Spokas et al., 2012). Biochar can also sequestrate carbon for many years due to the strong resistance of its aromatic carbon structure to biological decomposition (Lehmann et al., 2006). As listed in Table 1, detailed properties of rice straw biochar as a soil ameliorator were presented by Wu et al. (2012) for pyrolysis temperature of 300–700 °C. In pot trials for maize, using 1% mix of rice straw biochar with soil increased the growth of the crop by 64% (without fertilizer) and 146% (with fertilizer) (Peng et al., 2011). Application of wheat straw biochar to paddy fields achieved a significant increase in the rice yield and reduction in the overall greenhouse gas emission from the soil, especially in the second year of field experiment (Zhang et al., 2012).

In order to realize the potential benefits of biochar, it is essential to maximize its economic and environmental efficiency, including the production process of biochar. One important factor for the efficiency is how to utilize the by-products of biochar production. The amount of the bio-oil and non-condensable gas products in terms of mass and energy is considerably larger than that for biochar (Lee et al., 2013a). Bio-oil is a renewable fuel or chemical feedstock, but its chemical properties are not as good as biochar due to its high water content and numerous inhomogeneous compounds resulting in acidity and toxicity (Mohan et al., 2006). The pyrolytic gas is composed largely of CO and CO_2 that lead to poor fuel quality. Therefore, efficient use of the by-products should be considered together with biochar production, especially for large-scale production and application of biochar. This requires comprehensive information for mass yields and properties of the three pyrolysis products, including the distribution of carbon and chemical energy between products. However, such information is rare in slow pyrolysis studies in the literature, including those summarized in Table 1.

This study presents the slow pyrolysis characteristics of rice straw to provide comprehensive information for the chemical properties, carbon distribution and energy yields of the three pyrolysis products (biochar, bio-oil and gases). The mass yield, elemental composition and other key properties of the products were analyzed for pyrolysis temperatures of 300–700 °C. The carbon and energy yields of the products were calculated using analytical data. Based on these results, considerations required for application of the slow pyrolysis technology to rice straw were discussed.

2. Methods

2.1. Rice straw sample

The straw sample used in this study was from long grain rice delivered from Indonesia after air drying. Table 2 lists the chemical properties of the sample. Details of the analytical methods are presented in Section 2.3. The ash content was higher compared to the values in the literature (9.7–16.6%). Also, the volatile matter (VM) to fixed carbon (FC) ratio was lower in this sample, which can lead to larger char yields. However, the C, H, O, and N contents in the

Table 1
Recent studies on pyrolysis of rice straw reported in literature.

Refs.	Pyrolysis type	Reactor type	Temp. (°C)	Heating rate	Key results for products
Wannapeera et al. (2008)	Fast	Drop-tube, fixed-bed	200–850	>10^3 °C/s	Properties of char and gas; effect of holding time
Jung et al. (2008)	Fast	Fluidized	414–542		Product yields; properties of char, oil and gas
Zhang et al. (2013)	Fast	Fluidized; catalytic	550		Properties of oil
Eom et al. (2013)	Fast	Fluidized	350–500		Product yields; properties of oil
Pattiya and Suttibak (2012)	Fast	Fluidized	375–500		Product yields; properties of bio-oil
Fu et al. (2011, 2012)	Fast, slow	Quartz tube	600–1000	300 °C/s, 10 °C/min	Product yields; properties of char and gas
Lou et al. (2010)	Fast	Quartz tube	400–900	~10^4 °C/min	Product yields; properties of bio-oil and gas
Tu et al. (2009)	Plasma		467–603		Product yields; properties of char and gas
Pütün et al. (2004)	Slow	Fixed bed	400–650	5 °C/min	Product yields; properties of oil
Xiao et al. (2010)	Slow	Fixed bed	300–700	5 °C/min	Product yields; properties of char and oil
Peng et al. (2011)	Slow	Muffle furnace	250–450		Properties of biochar
Huang et al. (2012)	Slow	Microwave	237–423	13–31 °C/min	Properties of char (torrefaction)
Wu et al. (2012)	Slow	Tube furnace	300–700	5 °C/min	Properties of biochar
Chatterjee et al. (2013)	Slow	Fixed bed	500	10 °C/min	Properties of bio-oil (toxicity)
Huang et al. (2013)	Slow	Microwave	<550	~100 °C/min	Product yield; properties of gas

Table 2
Chemical properties of rice straw.

Biomass		Unit	This study	Literature[A]
Proximate analysis	Moisture	%air-dried	7.30	4.1–7.2
	VM[a]	%dry	60.84	
	FC[b,c]	%dry	16.61	
	Ash	%dry	22.55	9.7–16.6
	VM/FC		3.66	3.8–5.2
Ultimate analysis	C	%daf	48.75	41.8–54.3
	H	%daf	5.98	5.08–6.6
	O[c]	%daf	43.28	38.4–51.6
	N	%daf	1.99	0.4–3.9
Higher heating value (HHV)		$MJ/kg_{air\text{-}dried}$	13.45	15.0–16.2

[A] Pattiya and Suttibak (2012), Fu et al. (2011), Fu et al. (2012), Lou et al. (2010), Tu et al. (2009), Pütün et al. (2004), Xiao et al. (2010).
[a] Volatile matter.
[b] Fixed carbon.
[c] By difference.

organic fraction were within the ranges of the literature data. The higher heating value (HHV) was lower than those reported in the literature, attributable to the higher ash content. The difference in the analytical method could be one reason for the higher ash content compared to the literature, in addition to the variation of the feedstock. In this study, the ash content was measured by ASTM D1102-84. This requires gradual heating to 580–600 °C repeated by 30 min periods until the sample weight does not change (<0.2 mg). However, some studies (Huang et al., 2012) used ASTM D5142 for coal and coke that requires heating to 750 °C at the end of 1 h. The higher temperature and increased test duration may cause some loss of volatile inorganic compounds, such as K and Na, lowering the ash content. The difference caused by the two methods was about 1% for the sample. Many other studies did not specify the test method.

Cellulose, ranging from 34.4% to 44.0% in the literature, was the main component in the constitutional polymers of rice straw, while hemicellulose and lignin were similar in the range of 18–26%. Cellulose, hemicellulose and lignin are the three main organic polymers of land biomass. Their composition in biomass significantly influences the pyrolysis characteristics. Hemicellulose decomposes in the early stage of pyrolysis at a temperature range of 250–400 °C due to the chemical structures having weak bond strengths. This is followed by cellulose decomposition between 300 and 450 °C (Yang et al., 2007). Lignin is an amorphous, heavy molecular weight polymer containing aromatic carbons that slowly decomposes over a wide range of temperatures and contributes dominantly to the formation of char. The thermo-gravimetric analysis of the rice straw sample has been presented elsewhere (Lee et al., 2013b).

2.2. Slow pyrolysis

Slow pyrolysis tests were conducted using a lab-scale pyrolysis reactor for a target temperature of 300, 400, 500, 600 or 700 °C. The details of the reactor have been described elsewhere (Lee et al., 2013a). In each test, 100–110 g of the air-dried straw was placed in the reactor to be heated by an electric heater surrounding the reactor at a rate of 10 °C/min to a target temperature. Due to the heat consumed by evaporating moisture, the actual heating rate of the sample below 120 °C was lower than the target value. For the active heating period above 150 °C the heating rate increased to about 12 °C/min. Nitrogen was continuously supplied at a flow rate of 1.5 l/min to purge pyrolysis vapors from the reactor. Once the reactor attained the target temperature, it was maintained for 1 h for complete pyrolysis. The pyrolysis vapor containing condensable compounds (bio-oil) and non-condensable gases was passed through the bio-oil condensers and the gas analysis system. The connection tube from the reactor to the bio-oil condensers was heated at 350 °C by a band heater to prevent condensation of heavy compounds. The biochar and bio-oil collected after the test were collected and weighed to determine the mass yields. The composition of gases was continuously analyzed by an on-line gas analyzer (A&D System, A&D 9000) for CO and CO_2. The gases were also sampled to a gas chromatograph (Perkin-Elmer, Clarus 680 GC) every 9 min to determine CO, CO_2, H_2, CH_4, C_2H_4, C_2H_6, C_3H_6 and C_3H_8. The gas yield was calculated by difference. The pyrolysis test at each target temperature was repeated three times to determine the average mass yields of the three products. The deviations in the mass yields from the average were smaller than ±2.5% at 300 °C and ±0.5% at higher temperatures.

The mass yields on a wet basis ($Y_{i,wet}$) were converted into a dry, ash-free ($Y_{i,daf}$) basis to evaluate the product distribution from the organic fraction in biomass, as follows:

$$Y_{biochar,daf}\ (\%daf) = (Y_{biochar,wet} - A)/(100 - M - A) \times 100 \tag{1}$$

$$Y_{bio\text{-}oil,daf}\ (\%daf) = (Y_{bio\text{-}oil,wet} - M)/(100 - M - A) \times 100 \tag{2}$$

$$Y_{gas,daf}\ (\%daf) = Y_{gas,wet}/(100 - M - A) \times 100 \tag{3}$$

where M and A represent the moisture and ash contents in the raw material, respectively. The biochar yield was also converted to an ash-free basis to compare to data in the literature, as follows:

$$Y_{biochar,ash\text{-}free}\ (\%ash\text{-}free) = (Y_{biochar,wet} - A)/(100 - A) \times 100 \tag{4}$$

2.3. Analytical methods

The proximate analysis of raw biomass and biochar was based on the ASTM standards (moisture content: ASTM E871-82, ash: ASTM D1102-84, volatile matter: ASTM E872-82, and fixed carbon: calculated by difference). The ultimate analysis for C, H, and N content in the biomass, biochar and bio-oil fractions was performed using an elemental analyzer (CE Instruments, EA 1108), and the O content was calculated by difference. The heating value of the samples was measured by a bomb calorimeter (Parr Instrument, Parr-1261) for the higher heating value (HHV).

The bio-oil was a mixture of numerous hydrocarbons and water that was not in a homogenous solution. It gradually separated into two strata, of a light aqueous phase and dark heavy phase, during storage. The bio-oil collected from the condensation bottles was immediately separated into the two phases by a centrifuge for 15 min at 3000 rpm to minimize the effect of inhomogeneity on the property analysis. After separation and weighing, each phase was analyzed for the water content, elemental composition and heating value. The water content in the bio-oil was determined by Karl-Fisher titration (Metrohm, 870 KF Titrino plus). The overall properties of the bio-oil were then calculated by multiplying the weight fraction of each phase.

The biochar was further analyzed for pH, microscopic surface area and pore volume distribution. For the pH measurement, biochar to deionized water ratios of 1:20 (w:v) was used to form homogeneous suspension, and the pH was determined after 1.5 h of equilibration using an Orion PH meter (Thermo Scientific). The microscopic surface area of biochar was measured using the N_2-BET method (Micrometics, Tristar 3020). The surface morphology of biochar was investigated using scanning electron microscopy (SEM, JEOL JSM-7600F). The distribution of pore volumes in biochar was measured using a porosimeter (Micromeritics, AutoPore 4 9250) for the pores in the range of 10 nm–100 μm.

The above-mentioned analyses for the physical and chemical properties of raw biomass and pyrolysis products were performed at least three times per sample, and the average values were calculated.

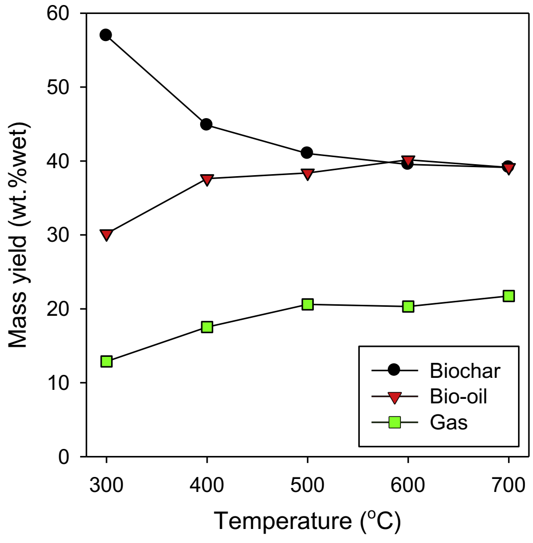

(a) Wet basis

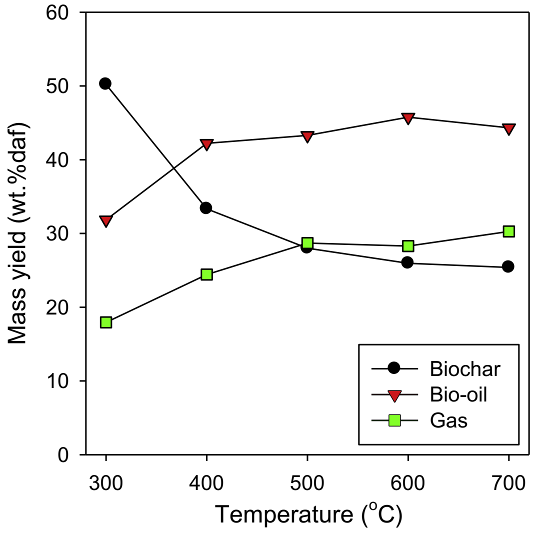

(b) Dry, ash-free basis

Fig. 1. Product yields from slow pyrolysis of rice straw.

3. Results and discussion

3.1. Product yields

Fig. 1 shows the product yields of pyrolysis for temperatures of 300–700 °C. The biochar yield decreased with temperature by the progress of thermal decomposition, resulting in gradual increases of bio-oil and gas yields. On a wet basis (Fig. 1a), biochar was the dominant product with a mass yield of over 39%. However, these yields included the contribution of ash that mostly remained in the solid residue. In contrast, the bio-oil yield included the contribution of moisture that was condensed in the oil collection bottles. After removing the influence of moisture and ash content using Eqs. (1)–(3), the product distribution showed noticeable changes. As shown in Fig. 1b, the bio-oil had the largest yield from the organic fraction (over 43.3%daf above 500 °C). The biochar yield rapidly decreased from 50.2%daf at 300 °C to 28.0%daf at 500 °C. The decrease above 500 °C was less than 2.6%daf, since the decomposition of cellulose and hemicellulose were completed. The bio-oil yield slightly decreased, while the gas yield increased at 700 °C. This could be understood from the cracking (secondary pyrolysis) of primary tar compounds by temperature and by hot char surface. Its effect was minor in this study, since the reactor was purged by nitrogen during heating. In a continuously-operating pyrolysis process where the tar compounds pass through hot char particles, the thermal/catalytic cracking could be significant above 600 °C and the carbon deposit remains on the biochar surface (Gilbert et al., 2009; Font Palma, 2013).

Fig. 2 compares the biochar yield to selected data in the literature. Considering the significant influence of ash and moisture content in the raw material, it was desirable to convert the biochar yield on a dry, ash-free basis. However, in many studies the basis of mass yields was not clearly stated or full analytical data were not given for the conversion. Therefore, the biochar yield on an ash-free basis was used instead, using Eq. (4). The yields of this study were about 3% lower than the results of Xiao et al. (2010) and Wu et al. (2012). In addition to the difference of feedstock properties and reactor configuration, a reason for the difference could be the rate of heating. While both studies used a rate of 5 °C/min, the value in this study was about 12 °C/min. Much higher rates further reduce the char yield, as shown for the fast pyrolysis tests of Lou et al. (2010) in Fig. 2.

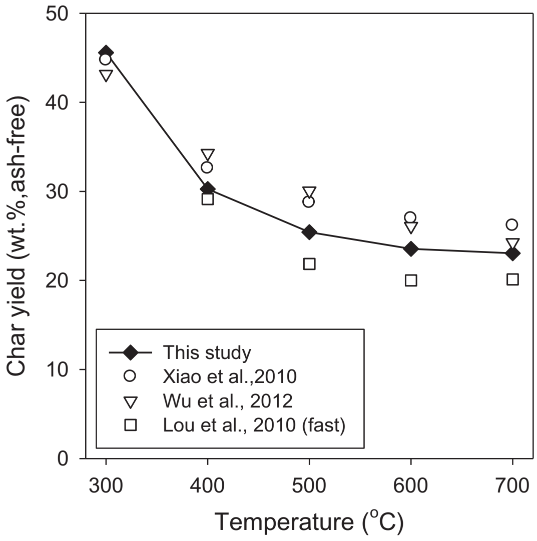

Fig. 2. Comparison of biochar yields on an ash-free basis with literature data.

3.2. Properties of biochar

Table 3 presents the summary of biochar properties. As the pyrolysis temperature increased, the biochar further released volatiles and became more carbonaceous. The loss of VM increased the relative proportion of the inert fraction (ash content) from 37.4%dry at 300 °C to 54.6%dry at 700 °C. This also led to a decrease in the HHV from 16.6 MJ/kg to 13.6 MJ/kg. Note that biochar exposed to air adsorbed some moisture ranging from 0.7% to 2.0%. This was excluded in the table.

The microscopic surface area of biochar indicates the adsorption capability for nutrients when applied to soil. The N_2-BET surface area for micro- and meso-pores (<50 nm) increased from 4.5 m^2/g at 300 °C to over 80 m^2/g at 600 °C. Similar values of surface area have also been reported in previous studies (Fu et al., 2011; Xiao et al., 2010). The decrease at 700 °C, which was confirmed by repeated analyses, could be the results of carbon deposit formation over the biochar surface from thermal and catalytic cracking of tar within the pyrolysis reactor. The surface area of the straw biochar was relatively low compared to biochar from a lignocellulosic biomass with a vascular structure. For example, the biochar from wood, sugar cane bagasse and miscanthus had over 100 m^2/g (Lee et al., 2013a,b) at 500 °C.

The pH of biochar increased from 9.0 at 300 °C to 10.5 at 500 °C and remained steady at higher temperatures. Wu et al. (2012) reported a similar range of pH values (9.3–10.9). The alkalinity of the rice straw biochar was mainly due to the presence of alkali metals in the inert biochar mass. Although Si was dominant (176,000 ppm), significant concentrations of K (21,340 ppm) and Na (753 ppm) were observed in the biochar at 500 °C (Lee et al., 2013b). The effects of decrease in acid functional groups, such as carboxyl (–COOH) and phenolic (–OH), would be minor on the alkalinity, since such groups became depleted with increasing pyrolysis temperature. The alkalinity of biochar is favorable for amelioration of acidic soils.

Fig. 3 compares the C, H and O composition of raw biomass and biochar on a van Krevelen diagram. The raw biomass was expressed in an empirical formula of $C_{1.00}H_{1.47}O_{0.67}N_{0.03}$. During pyrolysis, it rapidly released H and O atoms and approached the axis origin (pure carbon) with a trend line of (H/C) = 3.67(O/C). The data of Xiao et al. (2010) and Wu et al. (2012) also exhibited similar trends.

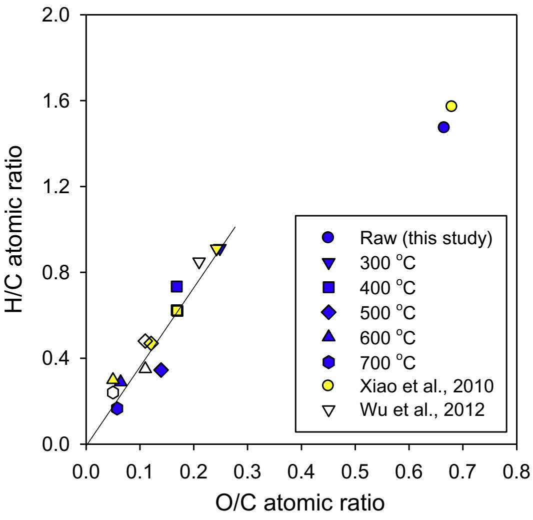

Fig. 3. Van Krevelen diagram for biochar from different pyrolysis temperatures.

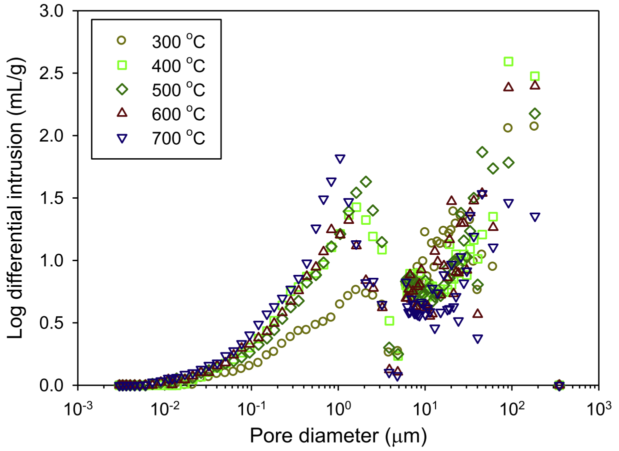

Fig. 4. Pore volume distribution of rice straw biochar.

Fig. 4 shows the distribution of pore volumes for a size range of 10 nm–100 μm. Two distinct size ranges, separated by a dip at 2–5 μm, were identified. The larger pores up to 100 μm originated from the vascular structure. The volume of the large pores was significant, even at 300 °C, since the pyrolysis already decomposed about 50% of the structural polymer into the volatiles (Fig. 1b), leaving the lignin-rich cell walls on the biochar. Further increase in the pore volume in this range was not noticeable at higher temperatures. These large pores are known to provide habitats for symbiotic micro-organisms in the soil (Thies and Rillig, 2009). The pore volume with a size of about 2 μm or smaller could be the result of pore formation on the surfaces of cell walls, which increased noticeably over 300 °C. The pore volumes in 10 nm or smaller were not well resolved in the porosimeter, but were found

Table 3
Summary of biochar properties from different pyrolysis temperatures.

Pyrolysis temperature (°C)		300	400	500	600	700
Proximate analysis (%dry)	VM	34.54	18.75	10.61	6.89	5.88
	FC[a]	28.06	35.39	38.72	39.87	39.52
	Ash	37.40	45.86	50.67	53.24	54.60
	VM/FC	1.23	0.53	0.27	0.17	0.15
Ultimate analysis (%daf)	C	68.72	75.47	81.43	87.52	91.15
	H	5.22	4.62	2.34	2.11	1.26
	O[a]	22.78	16.93	15.13	7.48	7.01
	N	3.28	2.98	1.10	2.89	0.58
HHV (MJ/kg-dry)		16.6	15.3	13.5	13.9	13.6
N_2-BET surface area (m^2/g)		4.5	21.2	45.8	84.8	22.5
pH		9.0	10.1	10.5	10.6	10.6

[a] By difference.

to be very small. This was in agreement with the low microscopic surface areas, as discussed previously.

3.3. Properties of bio-oil and gases

Table 4 summarizes the properties of bio-oil for the mass-weighted average of light aqueous and heavy organic phases. The aqueous phase accounted for 68–75% in the bio-oil with a water content as high as 82%. The overall elemental composition of the aqueous phase was C 13.1%, H 9.3%, O 76.3% and N 1.4% at 500 °C. The HHV of the aqueous phase was only about 3.7–4.4 MJ/kg due to the high water content. In contrast, the heavy organic phase was enriched with carbon and nitrogen, consisting of C 64.2%, H 8.2%, O 24.6% and N 3.0%. This led to a very high HHV (28.6–30.8 MJ/kg). In the overall properties of the bio-oil in Table 4, the bio-oil was higher in the oxygen content and the HHV ranged from 10.1 to 12.3 MJ/kg-wet.

Fig. 5 shows the profiles of gas concentration during a pyrolysis test at 600 °C. The symbols indicate the data measured by GC, while the lines for CO and CO_2 are from the on-line gas analyzer. C_{2+} represents the sum of C_2H_4, C_2H_6, C_3H_6 and C_3H_8. The release of CO_2 and CO was dominant in the early stage of pyrolysis, resulting mainly from the decomposition of cellulose and hemicellulose. Their concentration reduced rapidly above 400 °C, while H_2 and CH_4 gradually increased, mainly from the slow decomposition of lignin (Yang et al., 2007).

The gas release profiles for each test were integrated over the entire test duration to calculate the overall gas composition. For CO and CO_2, the gas analyzer data was used for integration. The remainder of gases was assumed linear between the data points from GC measured every 9 min. This assumption inevitably involved some error in the composition of H_2 and hydrocarbon gases. The error would be enlarged in the overall HHV of gases based on the integrated composition, since H_2 and hydrocarbons have very high HHVs (e.g., 141.80 MJ/kg for H_2 and 55.53 MJ/kg for CH_4) compared to CO (10.10 MJ/kg). Table 4 also shows the results of the gas composition and its heating value. CO_2 and CO remained as the dominant species throughout the tested temperature range, while the increases of CH_4 and H_2 were rapid above 400 °C. C_{2+} hydrocarbons peaked at 600 °C, which accounted for 0.68% C_2H_4, 1.75% C_2H_6, 0.57% C_3H_6 and 0.45% C_3H_8 at 600 °C in volume fractions. The contributions of H_2 and hydrocarbons to the HHV of the gas products were significant, as the value increased from 4.07 MJ/kg at 300 °C to 11.45 MJ/kg at 700 °C. Overall, the non-condensable gases were rich with oxygen-containing species, and had lower energy content than the biochar and bio-oil.

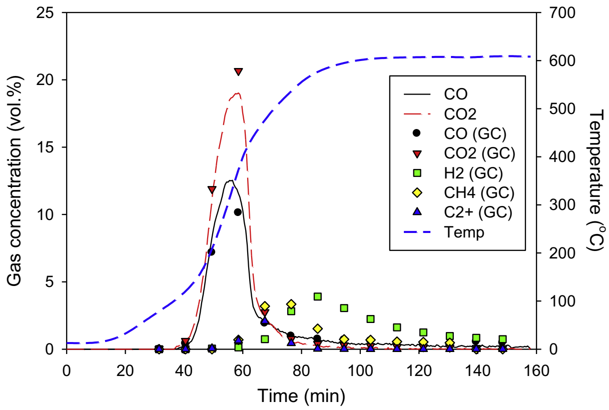

Fig. 5. Gas release profile during pyrolysis at 600 °C.

3.4. Carbon and energy distribution of the products

Fig. 6 shows the distribution of carbon and energy between pyrolysis products based on their mass yields, atomic compositions and HHV. For the carbon yield, biochar even at 700 °C retained 45% of carbon in the raw biomass. Therefore, biochar could be considered as the preferred product of carbon by pyrolysis that condensed the amorphous carbon structure with many functional groups and bridges into highly aromatic carbon skeletons. If the biochar applied to the soil remains without further decomposition, the equivalent CO_2 weight was about 59% (=$Y_{\text{biochar,wet}} \times C_{\text{biochar,dry}} \times 44/12$) of the air-dried biomass or 84% (=$Y_{\text{biochar,daf}} \times C_{\text{biochar,daf}} \times 44/12$) of its organic fraction above 500 °C. Bio-oil was the second important product, having carbon yields of 31.5–33.2% above 500 °C. The energy yield of biochar was about 40%, 5% lower than the carbon yield. The energy yield of bio-oil was comparable to that of biochar, since it contained more hydrogen-containing compounds. The pyrolytic gases had up to about 20% in both carbon and energy yields. The total carbon yields of the three products deviated by −2.2% to 3.2% from 100% by experimental errors that were insignificant. The deficiency of the total energy yield was larger, mainly due to the error involved in estimation of the gas composition and HHV.

Considering that the mass yield of biochar was about 25–28% over 500 °C, its carbon and energy yield of 40% or higher showed

Table 4
Composition of bio-oil and light gases (integrated) from pyrolysis.

Pyrolysis temperature (°C)			300	400	500	600	700
Bio-oil	Atomic composition (wt.%wet)	C	25.4	29.1	28.7	29.0	29.2
		H	10.1	9.3	8.9	8.4	8.4
		O	62.8	59.6	60.5	60.7	60.5
		N	1.8	2.0	1.9	1.9	1.9
	Atomic composition (wt.%dry)	C	33.5	36.1	35.5	35.4	35.9
		H	9.8	8.8	8.4	7.8	7.8
		O	54.5	52.6	53.8	54.5	54.0
		N	2.3	2.4	2.3	2.3	2.3
	HHV (MJ/kg-wet)		10.1	12.0	12.3	11.8	11.9
Light gases	Species composition (vol.%)	CO	43.2	38.7	33.6	28.8	26.3
		CO_2	54.1	52.8	50.0	38.7	33.1
		H_2	0.5	0.8	4.2	17.4	27.5
		CH_4	1.7	4.5	9.0	11.6	11.0
		C_{2+}	0.6	3.3	3.3	3.4	2.1
	Atomic composition (wt.%)	C	33.1	33.8	34.2	35.5	35.0
		H	0.3	1.1	1.9	3.6	4.5
		O	66.6	64.3	62.9	59.7	59.4
	HHV(MJ/kg)		4.1	5.8	7.1	10.3	11.4

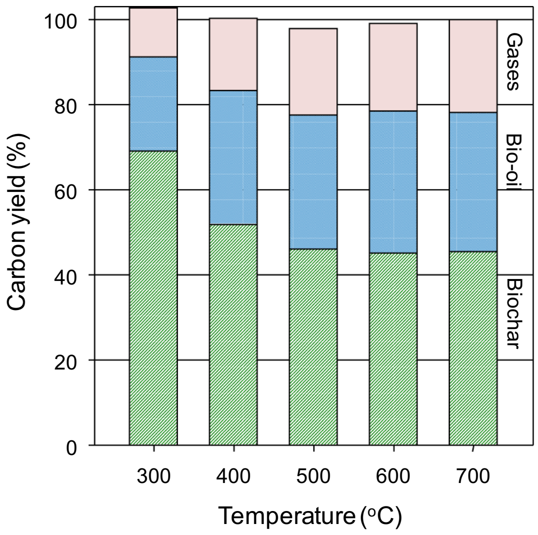

(a) Carbon yield

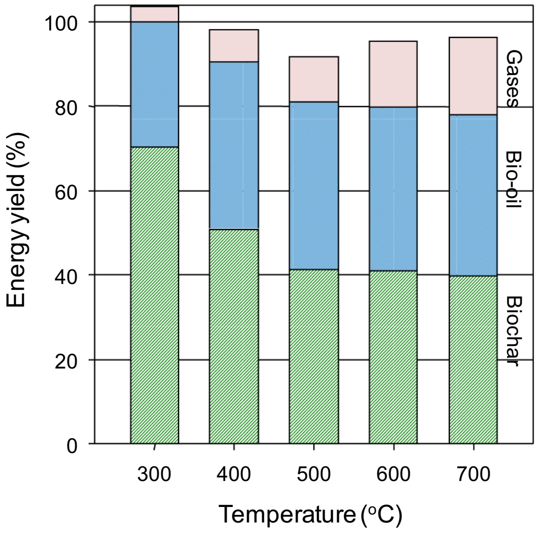

(b) Energy yield

Fig. 6. Carbon and energy distribution between pyrolysis products.

the value of biochar as a primary product of pyrolysis. It was also important to note that the by-products of biochar production, bio-oil and gases, contained 50–60% of carbon and energy content. Therefore, biochar production should be planned together with the utilization of by-products as valuable resources.

The gas product from pyrolysis can be burned to provide the heat on-site, since pyrolysis in an inert atmosphere requires external heat supply. Using the test results, the conditions for auto-thermal pyrolysis process with bio-oil collection can be evaluated. The heat required for pyrolysis (Q_{pyro}) of unit mass up to a temperature (T) can be estimated as the sum of enthalpy change of moisture (m_{water}) and dry mass fractions (m_{dry}) in the raw material, as follows:

$$Q_{pyro}\ (\mathrm{MJ/kg}) = m_{water}\Delta h_{water,T} + m_{dry}\Delta h_{dry,T} \tag{5}$$

where m_{water} = M/100 and m_{dry} = (100 – M)/100, $\Delta h_{water,T}$ can be directly calculated by the change in the specific enthalpy of water from the reference temperature (25 °C) to the target pyrolysis temperature including the latent heat. $\Delta h_{dry,T}$ represents the heat requirement for the dry mass or its products, incorporating the specific enthalpy and the endothermic heat of pyrolysis. In He et al. (2006), $\Delta h_{dry,T}$ measured for dry wheat straw was 0.558 MJ/kg up to 500 °C, and 0.568 MJ/kg up to 700 °C. However, this value was only for the remaining solid (char + ash), excluding the specific enthalpy of the volatile products leaving the solid. Therefore, it was simplified in this study to $\Delta h_{dry,T} = C_{p,avg}(T - 25)$ in which $C_{p,avg}$ was taken as 1.4 kJ/kg for approximation. Note that the ranges of C_p are typically 1.3–1.5 kJ/kg for dry biomass, 1.1–1.3 for char (Dupont et al., 2014), 0.9–1.1 for the inert fraction (mostly SiO_2) (Mills and Rhine, 1989) and 1.0–1.2 for light gases. In contrast, the heat released by combustion of gas products was calculated from the mass yield ($Y_{gas,wet}$) and its lower heating value (LHV_{gas}), as follows:

$$Q_{gas}\ (\mathrm{MJ/kg}) = Y_{gas,wet}\mathrm{LHV}_{gas} \tag{6}$$

Note that LHV was used in Eq. (6), since it represented the energy available without recovering the latent heat of H_2O in the combustion products.

Table 5 lists the values of Q_{pyro}, Q_{gas} and their ratio with different moisture content for pyrolysis at 400 °C and 600 °C. For pyrolysis at 400 °C, Q_{gas} is practically insufficient to provide Q_{pyro} and, therefore, a significant fraction bio-oil should be burned without condensation for the auto-thermal process. The heat required was 1.01 $\mathrm{MJ/kg_{straw}}$ for pyrolysis of air-dried straw at 600 °C, while the energy content in the gas product was sufficiently high (1.93 $\mathrm{MJ/kg_{straw}}$). The actual process would require an indirect heat exchange between biomass and hot combustion gas to maintain an inert atmosphere within the pyrolysis reactor. This would require an efficient heat exchanger design for increased heat recovery and compact reactor size. Q_{gas}/Q_{pyro} decreased rapidly to below 100% with an increase in moisture content. This was due to the increased heat demand for moisture evaporation, while the gas yield was reduced. The increased moisture content would also lower the heating value of bio-oil. Therefore, it was crucial to dry the rice straw as much as possible before feeding to a pyrolysis reactor.

4. Conclusions

Although the biochar yield from the organic fraction of rice straw was about 25–28%, its carbon and energy yields were about 40% or higher for pyrolysis above 500 °C. The volume of mesopores in the biochar was not large, which kept the specific surface area lower than 100 m^2/g. The high pH of biochar was attributable to the presence of alkali metals.

Table 5
Estimation of Q_{pyro}, Q_{gas} and their ratio for different moisture content.

Pyrolysis temperature	400 °C				600 °C			
Moisture content	7.3%[a]	10%	20%	30%	7.3%[a]	10%	20%	30%
Q_{pyro} ($\mathrm{MJ/kg_{straw}}$)	0.72	0.79	1.05	1.32	1.01	1.08	1.36	1.64
Q_{gas} ($\mathrm{MJ/kg_{straw}}$)	0.98	0.95	0.84	0.74	1.93	1.88	1.67	1.46
Q_{gas}/Q_{pyro}	136%	120%	80%	56%	192%	173%	122%	89%

[a] Air-dried condition.

Bio-oil and light gases contained about 50–60% of energy in total. The gases could be burned to provide the process heat for pyrolysis, but the drying of raw material was crucial for energy efficiency and bio-oil quality.

Acknowledgements

This work was supported by the Basic Science Research Program through the National Research Foundation of Korea (NRF) funded by the Ministry of Education, Science and Technology (Grant No. 2010-0006265).

References

Antal, M.J., Grønli, M., 2003. The art, science, and technology of charcoal production. Ind. Eng. Chem. Res. 42, 1619–1640.

Batidzirai, B., Mignot, A.P.R., Schakel, W.B., Junginger, H.M., Faaij, A.P.C., 2013. Biomass torrefaction technology: techno-economic status and future prospects. Energy 62, 196–214.

Chatterjee, N., Eom, H.J., Jung, S.-H., Kim, J.-S., Choi, J., 2013. Toxic potentiality of bio-oils, from biomass pyrolysis, in cultured cells and *Caenorhabditis elegans*. Environ. Toxicol. (in press) doi: 10.1002/tox.21871.

Dupont, C., Chiriac, R., Gauthier, G., Toche, F., 2014. Heat capacity measurements of various biomass types and pyrolysis residues. Fuel 115, 644–651.

Eom, I.-Y., Kim, J.-Y., Lee, S.-M., Cho, T.-S., Yeo, H., Choi, J.-W., 2013. Comparison of pyrolytic products produced from inorganic-rich and demineralized rice straw (*Oryza sativa* L.) by fluidized bed pyrolyzer for future biorefinery approach. Bioresour. Technol. 128, 664–672.

Font Palma, C., 2013. Modelling of tar formation and evolution for biomass gasification: a review. Appl. Energy 111, 129–141.

Fu, P., Yi, W., Bai, X., Li, Z., Hu, S., Xiang, J., 2011. Effect of temperature on gas composition and char structural features of pyrolyzed agricultural residues. Bioresour. Technol. 102, 8211–8219.

Fu, P., Hu, S., Xiang, J., Sun, L., Su, S., Wang, J., 2012. Evaluation of the porous structure development of chars from pyrolysis of rice straw: effects of pyrolysis temperature and heating rate. J. Anal. Appl. Pyrolysis 98, 177–183.

Gadde, B., Menke, C., Siemers, W., Pipatmanomai, S., 2008. Technologies for energy use of rice straw: a review. Int. Rice Res. Notes 33.

Gilbert, P., Ryu, C., Sharifi, V.N., Swithenbank, J., 2009. Tar reduction in pyrolysis vapours from biomass over a hot char bed. Bioresour. Technol. 100 (23), 6045–6051.

He, F., Yi, W., Bai, X., 2006. Investigation on caloric requirement of biomass pyrolysis using TG–DSC analyzer. Energy Convers. Manage. 47, 2461–2469.

Huang, Y.F., Chen, W.R., Chiueh, P.T., Kuan, W.H., Lo, S.L., 2012. Microwave torrefaction of rice straw and pennisetum. Bioresour. Technol. 123, 1–7.

Huang, Y.-F., Chiueh, P.-T., Kuan, W.-H., Lo, S.-L., 2013. Microwave pyrolysis of rice straw: products, mechanism, and kinetics. Bioresour. Technol. 142, 620–624.

Jahirul, M.I., Rasul, M.G., Chowdhurry, A.A., Ashwath, N., 2012. Biofuels production through biomass pyrolysis—a technological review. Energies 5, 4952–5001.

Jung, S.-H., Kang, B.-S., Kim, J.-S., 2008. Production of bio-oil from rice straw and bamboo sawdust under various reaction conditions in a fast pyrolysis plant equipped with a fluidized bed and a char separation system. J. Anal. Appl. Pyrolysis 82, 240–247.

Kim, S., Dale, B.E., 2004. Global potential bioethanol production from wasted crops and crop residues. Biomass Bioenergy 26, 361–375.

Lee, Y., Eum, P.-R.-B., Ryu, C., Park, Y.-K., Jung, J.-H., Hyun, S., 2013a. Characteristics of biochar from slow pyrolysis of Geodae-Uksae 1. Bioresour. Technol. 130, 345–350.

Lee, Y., Park, J., Ryu, C., Gang, K.S., Yang, W., Park, Y.-K., Jung, J., Huyn, S., 2013b. Comparison of biochar properties from biomass residues produced by slow pyrolysis at 500 °C. Bioresour. Technol. 148, 196–201.

Lehmann, J., Gaunt, J., Rondon, M., 2006. Bio-char sequestration in terrestrial ecosystems. Mitig. Adapt. Strat. Gl. 11, 403–427.

Lou, R., Wu, S., Lv, G., Guo, D., 2010. Pyrolytic products from rice straw and enzymatic/mild acidolysis lignin (EMAL). BioResources 5, 2184–2194.

Meng, J., Park, J., Tilotta, D., Park, S., 2012. The effect of torrefaction on the chemistry of fast-pyrolysis bio-oil. Bioresour. Technol. 111, 439–446.

Mills, K.C., Rhine, J.M., 1989. The measurement and estimation of the physical properties of slag formed during coal gasification, 2. properties relevant to heat-transfer. Fuel 68, 904–910.

Mohan, D., Pittman, C.U., Steele, P.H., 2006. Pyrolysis of wood/biomass for bio-oil: a critical review. Energy Fuels 20, 848–889.

Pattiya, A., Suttibak, S., 2012. Influence of a glass wool hot vapour filter on yields and properties of bio-oil derived from rapid pyrolysis of paddy residues. Bioresour. Technol. 116, 107–113.

Peng, X., Ye, L.L., Wang, C.H., Zhou, H., Sun, B., 2011. Temperature- and duration-dependent rice straw-derived biochar: characteristics and its effects on soil properties of an Ultisol in southern China. Soil Till. Res. 112, 159–166.

Pütün, A., Apaydın, E., Pütün, E., 2004. Rice straw as a bio-oil source via pyrolysis and steam pyrolysis. Energy 29, 2171–2180.

Spokas, K.A., Cantrell, K.B., Novak, J.M., Archer, D.W., Ippolito, J.A., Collins, H.P., Boateng, A.A., Lima, I.M., Lamb, M.C., McAloon, A.J., Lentz, R.D., Nichols, K.A., 2012. Biochar: a synthesis of its agronomic impact beyond carbon sequestration. J. Environ. Qual. 41, 973–989.

Thies, J.E., Rillig, M.C., 2009. Characteristics of biochar: biological properties. In: Lehmann, J., Joseph, S. (Eds.), Biochar for Environmental Management. Earthscan, Gateshead, UK, pp. 85–105 (Ch. 6).

Tu, W.-K., Shie, J.-L., Chang, C.-Y., Chang, C.-F., Lin, C.-F., Yang, S.-Y., Kuo, J.T., Shaw, D.-G., You, Y.-D., Lee, D.-J., 2009. Products and bioenergy from the pyrolysis of rice straw via radio frequency plasma and its kinetics. Bioresour. Technol. 100, 2052–2061.

Wannapeera, J., Worasuwannarak, N., Pipatmanomai, S., 2008. Product yields and characteristics of rice husk, rice straw and corncob during fast pyrolysis in a drop-tube/fixed-bed reactor. Songklanakarin J. Sci. Technol. 30, 393–404.

Wu, W., Yang, M., Feng, Q., McGrouther, K., Wang, H., Lu, H., Chen, Y., 2012. Chemical characterization of rice straw-derived biochar for soil amendment. Biomass Bioenergy 47, 268–276.

Xiao, R., Chen, X., Wang, F., Yu, G., 2010. Pyrolysis pretreatment of biomass for entrained-flow gasification. Appl. Energy 87, 149–155.

Yang, H., Yan, R., Chen, H., Lee, D.H., Zheng, C., 2007. Characteristics of hemicellulose, cellulose and lignin pyrolysis. Fuel 86, 1781–1788.

Zhang, A., Bian, R., Pan, G., Cui, L., Hussain, Q., Li, L., Zheng, J., Zheng, J., Zhang, X., Han, X., Yu, X., 2012. Effects of biochar amendment on soil quality, crop yield and greenhouse gas emission in a Chinese rice paddy: a field study of 2 consecutive rice growing cycles. Field Crop Res. 127, 153–160.

Zhang, H., Xiao, R., Jin, B., Shen, D., Chen, R., Xiao, G., 2013. Catalytic fast pyrolysis of straw biomass in an internally interconnected fluidized bed to produce aromatics and olefins: effect of different catalysts. Bioresour. Technol. 137, 82–87.